

Eosin-Y sensitized nanocrystalline TiO₂ Photoanode for Dye Sensitized Solar Cell application

M.T. Sarode^{1,*}, Y.B. Khollam², B.B. Kale³, P.N. Shelke⁴, K.C. Mohite⁵

¹Department of Physics, Mahatma Phule A.S.C. College, Panvel, 410206, India.

²Department of Physics, Baburaoji Gholap College, Sangvi, Pune 411027, India.

³Center for Material for Electronics Technology, Panchvati, Pashan, Pune 411008, India.

⁴Department of Physics, Anantrao Pawar College, Pirangut, Pune 412115, India.

⁵Department of Physics, C.T. Bora College, Shirur, Pune, 412210, India.

Abstract: For efficient charge injection and transportation, wide band gap nanostructured metal oxide semiconductor with dye adsorption surface and higher electron mobility are essential for photoanode in dye sensitized solar cells (DSSCs). In this study, TiO₂ films with anatase phase are prepared by using simple precipitation-annealing followed by cost effective Doctor's Blade method with titanium tetraisopropoxide as Ti-precursor. The influence of annealing temperature on structural, morphological, optical and photovoltaic properties is systematically investigated. The XRD and Raman spectroscopy characterization studies revealed the formation of pure single anatase phase TiO₂ in resultant films. The better optical properties: indirect band gap, absorbance coefficient and transmittance are found to be 3.19 eV, $1.70 \times 10^4/\text{cm}$ and 65.4 % respectively in resultant films. The better photovoltaic performance: open circuit voltage (V_{oc}) = 0.564 V, current density (J_{sc}) = 4.80 mA/cm², fill factor (FF) = 42.57 % and photo conversion efficiency = 1.03 % using Eosin-Y dye with polyiodide electrolyte is obtained for DSSC of nanocrystalline TiO₂ films obtained at 400 °C.

Keywords: TiO₂; Nanomaterial; Doctor's Blade method; Eosin-Y dye; DSSC.

1. Introduction

In modern day of research, wide band gap semiconductors have been studied intensively due to their potential applications in many areas, such as sensors, laser diodes, high speed electronic devices etc. [1-3]. TiO₂ has attracted considerable attention owing to its wide band gap [4]. Thin films of TiO₂ have been studied widely in recent years for many applications like environmental applications, photocatalysis, electrochromic devices and photovoltaic cells [5-7] because of their better biocompatibility, thermal stability, strong oxidized stability, non-toxicity and long term photo-stability. It is also used in non-electronic applications like optical brightener in wall colors, ingredient in sun cream and bone implants [8]. TiO₂ thin films have been deposited by many researchers by using different techniques like, molecular beam epitaxial, chemical vapor deposition, aerosol pyrolysis, electrodeposition and sol-gel method [9-10]. In present study, TiO₂ films with anatase phase are prepared by using simple precipitation-annealing followed by cost effective Doctor's Blade method with titanium tetra isopropoxide as Ti-precursor. The photovoltaic properties of inexpensive Eosin-Y dye sensitized solar cells of resultant anatase phase pure TiO₂ films are recorded. The data pertaining to this is presented in this communication.

2. Experimental

2.1. Synthesis of TiO₂ powder

A 25 ml of titanium tetra-isopropoxide (TTIP) (Spectrochem Chem., AR grade) was slowly added to 100 ml of double distilled water (DDW). This hydrolysis was carried out in an ice bath under vigorous stirring. The resultant white precipitate was washed with double distilled water for by using centrifuge. Then precipitate was dried at 80 °C for 1 hr. The as-dried precipitate was annealed at 300, 400 and 500 °C for 2 hr to obtain TiO₂ powders.

2.2. Preparation of TiO₂ films

Indium tin oxide (ITO) glass substrates were washed with detergent and double distilled water. Then substrates were boiled in concentrated chromic acid (0.5 M) for 1 hr and kept in it for 5 hr. Then substrates were rinsed with double distilled water. Lastly, substrates were cleaned ultrasonically in acetone for 15 min. and then dried under IR lamp. The 0.50 gm of as-prepared TiO₂ powder was mixed with 0.25 gm of polyethylene glycol (PEG, M.W. 20,000) by using pestle-mortar in dilute acetic acid medium to produce a lump free paste. Three edges of thoroughly cleaned ITO substrate were masked with TISCO tape by keeping the 1 cm² area free for the deposition of film. The thickness of tape loaded over the substrate was between 10 -11 μm. The unmasked region of ITO substrate was completely filled with the lump free paste of TiO₂ by using Doctor's Blade method. This film was dried under halogen lamp for 30 min. The resultant films were characterized by using different physical techniques. The X-ray diffraction patterns of resultant films were recorded by using Bruker D8 Advance (filtered CuK_α radiation, λ = 1.5406 Å) machine. Raman spectra were recorded by Jobin Yvon Horibra LABRAM-HR (single mode Ar-ion laser for excitation λ = 488 nm) spectrometer. The average thickness of the films measured by using surface profiler (KLA Tencor P -16+) was found to be 10.23 μm. The optical spectra of films were recorded by using the UV-Visible spectrophotometer (V-670, JASCO UV-VIS-NIR spectrometer). The surface morphology was determined by using scanning electron microscope (JEOL JSM-6360-LA and Philips XL-30). Finally, the resultant films were subjected for the fabrication of dye sensitized solar cells (DSSCs).

2.3. Fabrication of dye sensitized solar cell

The resultant film was used for fabrication of dye sensitized solar cell (DSSC). The resultant film was immersed in 0.3 mM solution of Eosin-Y dye in ethanol for 24 hr. Then film was rinsed with DDW and acetonitrile to remove excess amount of dye and dried at room temperature. This dye loaded film was further used as working electrode. The carbon coated ITO glass substrate was used as a counter electrode. The counter electrode was clamped on the top of working electrode to form solar cell. The few drops of redox (I⁻/I₃⁻) electrolyte solution of polyiodide (1 M KOH + 1 M KI + 0.5 M iodine) in acetonitrile were poured from exposed side of DSSC. The solution gets absorbed into DSSC by capillary action. The current density (J)- voltage (V) curves were recorded immediately after fabrication for different DSSCs (area = 0.25 cm²) at the input power = 1000 W/m² of incident light from neon lamp by using solar simulator (Newport Corporation's Oriol® Sol2A® Class ABA solar simulation systems). The J-V curves were used to obtain the photovoltaic properties of DSSCs.

3. Results and discussion

3.1. X-ray diffraction

The X-ray diffraction (XRD) patterns of films obtained at different temperatures are shown in fig. 1(a). The diffraction patterns display crystalline nature with simultaneous presence of broad hump in low 2θ region demonstrating its short range order. The diffraction pattern of film obtained at 300 °C exhibits broad hump with two peaks. The diffraction patterns of films obtained at 400 and 500 °C show distinct peaks with low intensities. The peaks are indexed to the anatase of TiO₂. The diffraction peaks (101), (004), (200) and (105) corresponding to the anatase TiO₂ phase are observed in the XRD patterns of films obtained at 400 and 500 °C films. The peaks corresponding to the rutile phase of TiO₂ are not seen in the XRD patterns suggesting clearly that only anatase phase is formed in resultant films. The peaks positions and their relative intensities are noted to be consistent with the standard powder diffraction pattern of anatase TiO₂. The crystallite size for the films obtained at 300, 400 and 500 °C is determined from the integral width of the (101) plane by using Scherrer's formula [11]. The data for crystallite size, interplaner spacing d, lattice parameter (a = b and c) and unit cell volume for TiO₂ particles of resultant films are given in Table 1. The crystallite size is found to be increasing with increasing annealing temperature and its average value is 16.98 nm. The annealing at higher temperature facilitates the subsequent crystal growth process accompanied by the diffusion of titania species towards nucleated grains resulting in grain growth. The data for d₁₀₁ spacing and lattice parameter are found to be matching with reported data.

Table 1: Structural properties of resultant films

Temperature (°C)	Crystallite size (nm)	d ₁₀₁ spacing (nm)		Phase symmetry	Lattice parameter (nm)		Unit cell volume (nm ³)
		observed	standard		a = b	c	
300	15.24	0.3534	0.3520	Anatase	0.3778	0.9496	0.1368
400	17.34	0.3543	0.3520	Anatase	0.3779	0.9497	0.1344
500	18.36	0.3556	0.3520	Anatase	0.3786	0.9498	0.1368

3.2. Raman spectroscopy

Raman spectra of the films obtained at 300, 400 and 500 °C are shown in fig. 1 (b). Raman spectra with well defined peaks and absence of overlapping peaks confirm that the films are well crystallized with low number of imperfect sites.

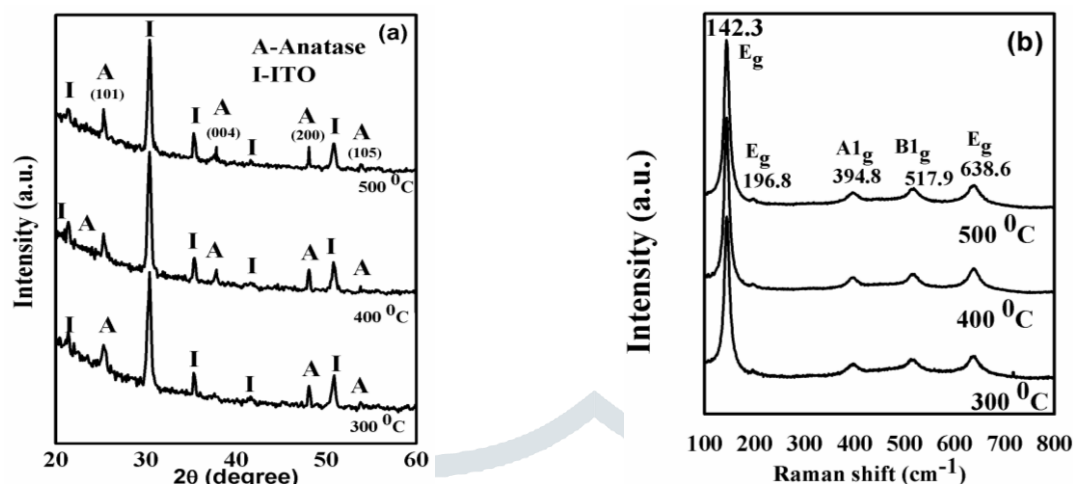


Fig. 1 (a) X-ray diffraction patterns and (b) Raman spectra of resultant films obtained different temperatures

The anatase TiO₂ has six Raman active modes: A_{1g}, 2B_{1g}, and 3E_g. For TiO₂ single crystal, the following allowed bands: $142 \pm 2 \text{ cm}^{-1}$ (E_g), $194 \pm 3 \text{ cm}^{-1}$ (E_g), $393 \pm 2 \text{ cm}^{-1}$ (B_{1g}), $512 \pm 1 \text{ cm}^{-1}$ (A_{1g}), $519 \pm 1 \text{ cm}^{-1}$ (B_{1g}) and $634 \pm 2 \text{ cm}^{-1}$ (E_g) are reported [12]. The five distinct peaks [fig. 1 (b)] are observed in the Raman spectra of all films, which can be assigned according to the above-given allowed modes of anatase. The observed peaks have bands centered at 142.3 cm^{-1} (E_g), 196.8 cm^{-1} (E_g), 394.8 cm^{-1} (B_{1g}), 517.9 cm^{-1} (A_{1g}) and 638.6 cm^{-1} (E_g). The absence of peaks corresponding to rutile phase in the Raman spectra confirms the formation of pure anatase TiO₂ [13].

3.3. Scanning electron microscopy

The scanning electron microscopy (SEM) images of films obtained at 300, 400 and 500 °C are shown in fig. 2. The SEM images show the following general observations: (i) primary particles are nearly spherical, (ii) particle size distribution of primary particles is nearly uniform and (iii) nature of particles is soft/hard agglomerates. The soft agglomerates with varied bigger size and shapes are observed in film obtained at 300 °C. Further, the hard agglomerates with varied shapes and nearly uniform size distribution are seen in film obtained at 500 °C. However, spherical soft agglomerates with uniform particle size distribution are found in the film obtained at 400 °C.

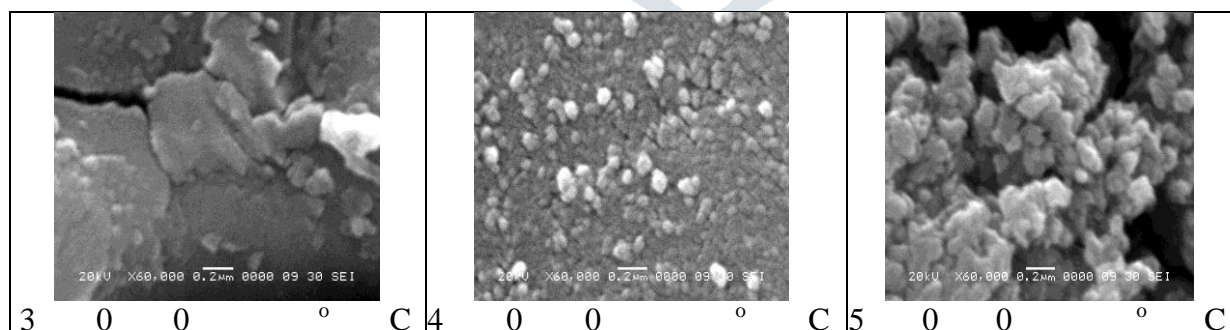


Fig. 2. Scanning electron microphotographs of resultant films obtained different temperatures

3.4. Optical band gap

Fig. 3(a) gives the UV-Visible transmittance spectra for the resultant films. Tauc's plots [14] generated from the UV-Visible spectra for resultant films are given in fig. 3(b) to obtain the indirect band gap energy (E_g).

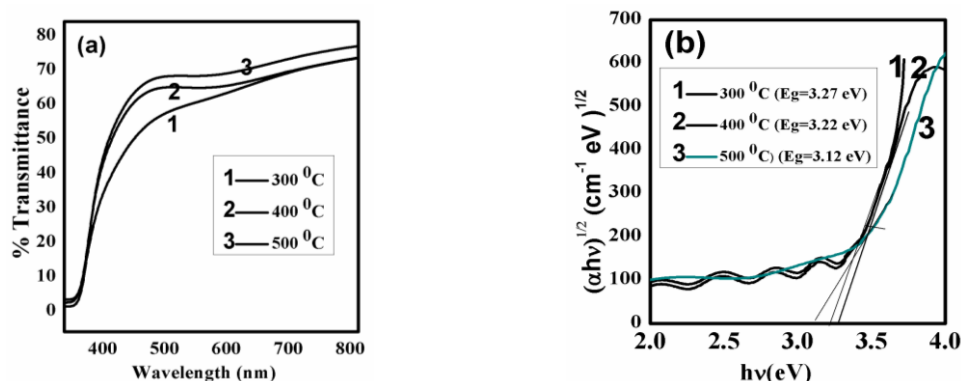


Fig. 3 (a) UV- Visible transmittance spectra and (b) variation of $(\alpha hv)^{1/2}$ vs. hv (indirect band gap) for resultant films obtained different temperatures

The value of E_g is obtained by extrapolation of straight-line portion of the plot to zero absorption edge. Further, the absorption coefficient is obtained by using relation: $\alpha = \ln(1/T)/d$, where, d = thickness of film and T = % transmittance of the film. The optical properties of films are given in Table 2. The thickness of the film is seen to be decreasing at higher annealing temperature. This is due to densification of film at higher annealing temperature. The average film thickness is found to be 10.23 μm . Further, due to decreasing thickness the transmittance is found to increasing with the annealing temperature. The band gap is found to be matching with the reported data. The absorption coefficient, α is found to be maximum for the film obtained at 400 $^{\circ}\text{C}$.

Table 2. Optical properties of resultant films obtained different temperatures

Temperature ($^{\circ}\text{C}$)	Thickness (μm)	% T at $\lambda = 550$ (nm)	Indirect band gap (E_g) eV	Absorption coefficient (α) $\times 10^4 \text{ cm}^{-1}$
300	10.4	56.2	3.27	0.97
400	10.2	60.1	3.20	1.70
500	10.1	65.4	3.12	1.20

3.5. Photovoltaic properties

Fig. 4 shows the current density (J) vs. voltage (V) curves for the DSSCs of different resultant films. The data obtained for various solar cell parameters is summarized in Table 3. The photovoltaic performance of these dye sensitized solar cells by using inexpensive Eosin-Y dye is noted to be better as compared to the data reported with costly dyes. The maximum photovoltaic performance of DSSC of film obtained at 400 $^{\circ}\text{C}$ might be due to lowest - uniform particle size distribution and high absorption coefficient of corresponding TiO_2 film.

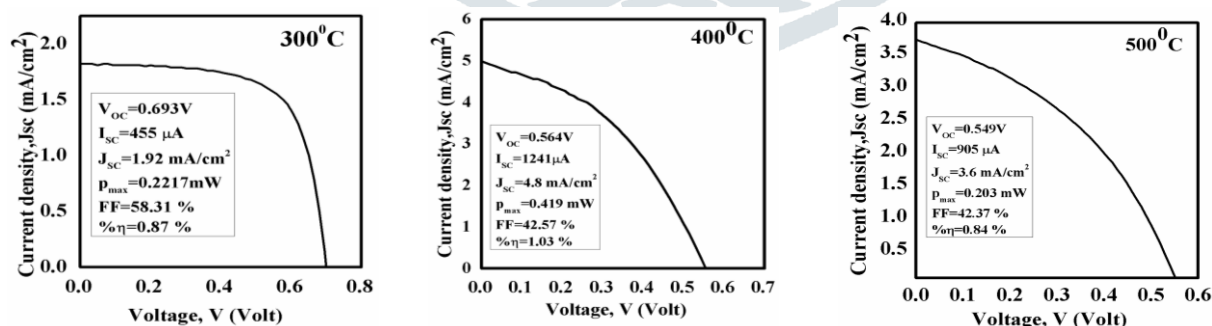


Fig. 4 J-V curves for resultant films

Table 3 Photovoltaic properties for DSSCs of resultant films

Parameter	TiO ₂ film obtained at		
	300 $^{\circ}\text{C}$	400 $^{\circ}\text{C}$	500 $^{\circ}\text{C}$
Open circuit voltage, V_{oc} (volt)	0.693	0.564	0.549
Short circuit current, I_{sc} (mA)	455	1241	905
Maximum voltage, V_{max} (volt)	0.271	0.400	0.405

Maximum current I_{\max} (μA)	723	987	491
Maximum power P_{\max} (mW)	0.221	0.419	0.203
Current density, J_{sc} (mA/cm^2)	1.91	4.80	3.60
Fill factor, FF (%)	58.31	42.57	42.37
Efficiency, η (%)	0.87	1.03	0.84
Seris resistance, R_s (Ω)	2264.62	2135.15	2154.15
Shunt resistance, R_{SH} ($\text{k}\Omega$)	241.76	87.63	109.782

4. Conclusions

Doctor's Blade technique is simple, inexpensive and versatile route for the preparation of films. The TiO_2 films prepared in present work by using simple precipitation-annealing followed by Doctor's Blade technique showed formation of nano-crystalline phase pure TiO_2 particles with anatase symmetry. The annealing temperature is found to have profound effect on photovoltaic performance of DSSCs of resultant TiO_2 films. The better solar cell characteristics: $V_{\text{oc}} = 0.564$ V, $J_{\text{sc}} = 4.8$ mA/cm^2 , $\text{FF} = 42.57$ % and $\eta = 1.03$ % using Eosin -Y dye with polyiodide electrolyte are obtained for the DSSC of the TiO_2 film obtained 400 °C. This might be due to lowest - uniform particle size distribution and high absorption coefficient of corresponding TiO_2 film.

Acknowledgment

The author MTS is thankful to Principal Dr. Arun Andhale, M.P.A.S.C. College, Panvel, India, Director, School of Energy Studies, Savitribai Phule Pune University, Pune, India and Centre for Materials for Electronics Technology (C-MET), Pune for providing research facilities to the present work.

References

- [1] M. A. Haase, J. Qiu, J. M. Depugdt, H. Cheng, Appl. Phys. Lett., 59 (1991) 1272.
- [2] S. D. Lester, F. A. Ponce, M. G. Gerafordand, D. A. Steigerwald, Appl. Phys. Lett., 66 (1995) 1249.
- [3] R. F. Serice, Science, 276 (1997) 895.
- [4] A. R. Gandheand, J. B. Fernandes, Bull. Catal. Soc. India, 4 (2005) 131.
- [5] X. Quan, S. Yang, X. Ruan, H. Zhao, Environ. Sci. Technol., 39 (2005) 3770.
- [6] S. Livraghi, A. Votta, M. C. Paganniniand, E. Giamello, Chem. Commun., 4 (2005) 498.
- [7] O. K. Varghese, D. W. Gong, M. Paulose, K. G. Ong, E. C. Dickeyand, C. A. Grimes, Adv. Mater., 15 (2003) 624.
- [8] A. Welte, C. Waldanf, C. Brabee, P. J. Wellmann, Thin Solid Films, 516 (2008) 7256.
- [9] C. J. Barbe, F. Arendse, F. Arendse, P. Comte, M. Jirousek, F. Lenzmann, V. Shklover, M. Gratzel, J. Am. Ceram. Soc., 80 (1997) 3157.
- [10] J. Xu, X. Zhao, J. Duand, W. Chen, J. Sol - Gel Sci. Technol., 17 (2000) 163.
- [11] W. Que, A. Uddinand, X. Hu, J. Power Sources, 159 (2006) 353.
- [12] T. Ohsaka, Y. Izumi, Y. Fujiki, J. Raman Spectrosc., 7 (1978) 321.
- [13] Y. Djaoved, S. Badilescu, P. Vashirt, J. Robichaud, Int. J. Vib. Spectrosc., 5 (2002) 4.
- [14] P. Chrysicopoulou, D. Davazoglou, C. Trapalis, G. Kordas, Thin Solid Films, 323 (1998) 188.